Mathematics and Computer Science   College of Arts & Sciences

Numerical analysis of coupled systems of ODEs and applications toenzymatic competitive inhibition by product

Vinh Quang Mai

Thái Ahn Nhan
Santa Clara University, anhan@scu.edu

Recommended Citation

Mai, V. & Nhan, T. A. (2021). Numerical analysis of coupled systems of ODEs and applications to enzymatic competitive inhibition by product. Advances in the Theory of Nonlinear Analysis and its Application, 5 (1), 58-71. doi.org/10.31197/atnaa.820590

Numerical analysis of coupled systems of ODEs and applications to enzymatic competitive inhibition by product

Vinh Quang Mai[a], Thái Anh Nhan[b]

[a]*Department of Mathematics, Thu Dau Mot University, Binh Duong, Vietnam.*
[b]*Department of Mathematics and Science, Holy Names University, Oakland, CA 94619, USA.*

Abstract

Enzymatic inhibition is one of the key regulatory mechanisms in cellular metabolism, especially the enzymatic competitive inhibition by product. This inhibition process helps the cell regulate enzymatic activities. In this paper, we derive a mathematical model describing the enzymatic competitive inhibition by product. The model consists of a coupled system of nonlinear ordinary differential equations for the species of interest. Using nondimensionalization analysis, a formula for product formation rate for this mechanism is obtained in a transparent manner. Further analysis for this formula yields qualitative insights into the maximal reaction velocity and apparent Michaelis-Menten constant. Integrating the model numerically, the effects of the model parameters on the model output are also investigated. Finally, a potential application of the model to realistic enzymes is briefly discussed.

1. Introduction

Enzymes are biocatalysts naturally present in living organisms. Enzymes are capable of increasing the rates of the chemical reactions by reducing the activation energy of reactions [1, 2]. They are usually involved

Email addresses: `vinhmq@tdmu.edu.vn` (Vinh Quang Mai), `nhan@hnu.edu` (Thái Anh Nhan)

in cellular metabolism to produce the metabolites needed for the cells . Cells use many regulatory mechanisms to regulate the concentrations of metabolites at physiological levels. Enzymatic inhibition processes are very common mechanisms in cellular metabolism [3, 4].

There are three main inhibition processes of enzymes and they are competitive inhibition, allosteric (non-competitive) inhibition, and uncompetitive inhibition processes. In the competitive inhibition process, the enzyme molecule has one binding site for the substrate and inhibitor. Inhibitor molecules compete with substrate molecules for the binding sites of enzyme molecules. The binding of a inhibitor molecule to an enzyme molecule prevents the substrate molecules from binding to the enzyme molecule and form an enzyme-inhibitor complex, so this enzyme molecule is not able to catalyse reactions to form product. Competitive product inhibition of an enzyme is an competitive inhibition process in which the product plays the role of inhibitor [3, 4, 5]. Mini-hexokinase I is one of the enzymes that are inhibited by their products [6, 7].

Figure 1 graphically depicts the enzymatic reactions for the kinetic mechanism of competitive product inhibition of an enzyme. In the model, the enzyme molecule has one binding site that can accommodate both the substrate and the product. When the product of the active site binds to the binding site, it prevents the substrate molecules from binding to the binding site. A minimal set of chemical reactions representing competitive product inhibition is given by

$$
\begin{aligned}
S + E &\underset{k_{-1}}{\overset{k_1}{\rightleftharpoons}} ES \xrightarrow{k_0} E + P, \\
P + E &\underset{k_{-2}}{\overset{k_2}{\rightleftharpoons}} EP,
\end{aligned}
\tag{1}
$$

where E, S, and P denote an enzyme molecule, a substrate molecule, and a product molecule, respectively. The complexes ES and EP have the obvious interpretation; see Figure 1.

It is well known that the Michaelis-Menten formula for the product formation rate of enzymatic reactions is derived from a simple model for the kinetic mechanism of an enzyme, and it is a widely used tool in studying the kinetic mechanism of enzymes [5].

The remainder of this paper is organised as follows. In Section 2, we describe the formulation of the mathematical model. The non-dimensionalization analysis of the model is described in Section 3, and the effects of the model parameters on the product formation rate are given in Section 4. In Section 5, an application of the model to the phosphorylation of glucose by mini-hexokinase I is briefly introduced. Finally, we finish with several conclusions in Section 6.

2. The mathematical model

In this section, we develop a minimal model that describes the kinetic mechanism of competitive product inhibition of an enzyme. The model is based on the mechanism described in Section 1. Although the formula for the product formation rate is already available in the literature [8, 9, 10], we shall derive it in a transparent manner by non-dimensionalising the equations and making rational approximations. We begin by listing our modelling assumptions.

2.1. Modelling assumptions

(i) It is assumed throughout that the mixture of substrate and enzyme is well-stirred. This implies that diffusive effects in the degradation process can be neglected, and that the concentrations of the various species in the mixture can be described by functions of time only. This further implies that the evolution of the system can be modelled by a coupled system of nonlinear ordinary differential equations, and that a partial differential equations model is not required [11].

(ii) We assume mass action kinetics throughout; this implies that the rate of a reaction is taken to be proportional to the product of the concentrations of the reactants. We emphasize here that more complex formulas, such as the MichaelisâĂŞMenten formula for the rate of product production in an enzyme-catalysed reaction, are derivable from more fundamental mass action considerations under simplifying assumptions [5, 11].

NOMENCLATURE

$[X]$ − the concentration of a species X; a function of time (mM)

E − a molecule of the enzyme

S − a molecule of the substrate

ES − an enzyme-substrate complex

EP − an enzyme-product complex

P − a molecule of the product

k_0 − catalytic rate for the enzyme acting on a substrate molecule (s^{-1})

k_1 − adsorption rate of substrate molecules to free enzyme molecules $(mM^{-1}s^{-1})$

k_{-1} − desorption rate of substrate molecules from enzyme-substrate complexes (s^{-1})

k_2 − adsorption rate of product molecules to free enzyme molecules $(mM^{-1}s^{-1})$

k_{-2} − desorption rate of product molecules from enzyme-product complexes (s^{-1})

2.2. The governing ordinary differential equations

Applying the law of mass action in the usual way, the corresponding governing ordinary differential equations are given by

$$\frac{d[E]}{dt} = -k_1[E][S] - k_2[E][P] + k_0[ES] + k_{-1}[ES] + k_{-2}[EP], \tag{2a}$$

$$\frac{d[ES]}{dt} = -(k_0 + k_{-1})[ES] + k_1[E][S], \tag{2b}$$

$$\frac{d[EP]}{dt} = -k_{-2}[EP] + k_2[E][P], \tag{2c}$$

$$\frac{d[S]}{dt} = -k_1[E][S] + k_{-1}[ES], \tag{2d}$$

$$\frac{d[P]}{dt} = -k_2[E][P] + k_0[ES] + k_{-2}[EP], \tag{2e}$$

where $[X] = [X](t)$ denotes the concentration of species X at time t.

It is not necessary to discuss all of these equations here. However, we do briefly discuss two of them to illustrate how the governing equations are constructed. The chemical reactions for the model are displayed in Figure 1. We begin by considering the equation for S. This is given by

$$\frac{d[S]}{dt} = \overbrace{-k_1[E][S]}^{\text{ⓐ}} + \overbrace{k_{-1}[ES]}^{\text{ⓑ}},$$
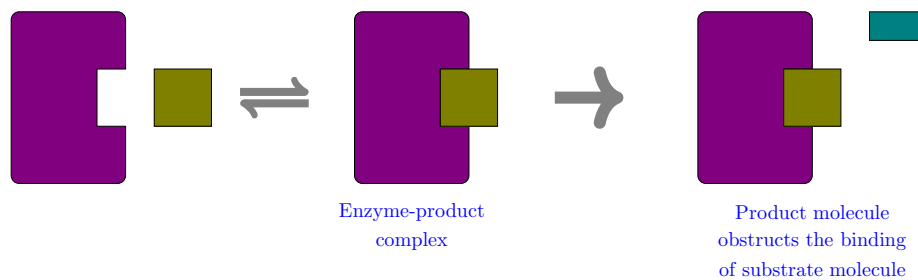
where
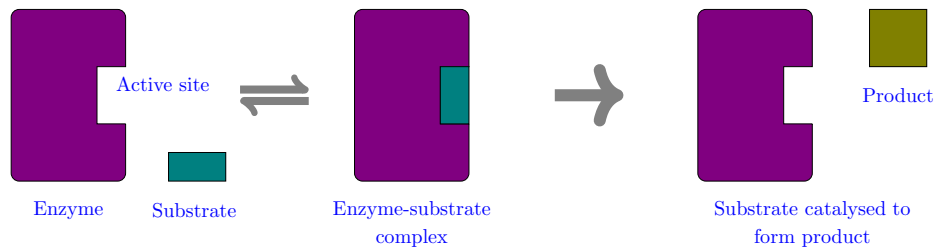
(a) Reaction

(b) Inhibition

Figure 1: Diagram of reactions and inhibition. The enzyme here has one binding site that can accommodate both the substrate and the product. In (a) a substrate binds to a free enzyme molecule to form an enzyme-substrate complex. The enzyme then catalyses the substrate to form a product. In (b) binding of a product molecule to a free enzyme molecule to form an enzyme-product complex prevents the enzyme molecule from binding with a substrate.

ⓐ - this term accounts for the reduction in concentration of S due to enzyme binding.

ⓑ - the increase in concentration of S due to enzyme unbinding from the complex ES.

Next consider the equation for the enzyme E, given by

$$\frac{d[E]}{dt} = \overbrace{-k_1[E][S]}^{①} \overbrace{-k_2[E][P]}^{②} + \overbrace{k_0[ES]}^{③} + \overbrace{k_{-1}[ES]}^{④} + \overbrace{k_{-2}[EP]}^{⑤},$$

where

① - this term accounts for the reduction in concentration of E due to enzyme binding to the substrate S.

② - the reduction in concentration of E due to enzyme binding to the product P.

③ - the increase in concentration of E due to enzyme catalysing the complex ES and releasing the product then.

④ - the increase in concentration of E due to enzyme unbinding from the complex ES.

⑤ - the increase in concentration of E due to enzyme unbinding from the complex EP.

The remaining equations (2b), (2c), and (2e) are interpreted similarly. These equations are to be solved subject to the initial conditions

$$[E](t=0) = e_0,$$
$$[S](t=0) = s_0,$$
$$[ES](t=0) = 0,$$
$$[EP](t=0) = 0,$$
$$[P](t=0) = 0,$$

where e_0, s_0 are positive constants corresponding to the initial concentrations of enzyme and substrate, respectively. Summing the first three equations, (2a) + (2b) + (2c), in (2) and integrating yields

$$[E] + [ES] + [EP] = e_0, \tag{3}$$

which is an expression of conservation of enzyme.

3. Nondimensionalization analysis

We non-dimensionalize the equations by introducing the dimensionless variables

$$e = \frac{[E]}{e_0}, \ c_1 = \frac{[ES]}{e_0}, \ c_2 = \frac{[EP]}{e_0}, \ s = \frac{[S]}{s_0}, \ p = \frac{[P]}{s_0}, \ \tau = e_0 k_1 t.$$

The governing equations may be written in the equivalent dimensionless form

$$\varepsilon \frac{dc_1}{d\tau} = -(s + \hat{k}_0 + \hat{k}_{-1})c_1 - sc_2 + s, \tag{4a}$$

$$\varepsilon \frac{dc_2}{d\tau} = \hat{k}_2 \left(-pc_1 - (p + \hat{k}_{-2}/\hat{k}_2)c_2 + p \right), \tag{4b}$$

$$\frac{ds}{d\tau} = \hat{k}_{-1}c_1 - s(1 - c_1 - c_2)), \tag{4c}$$

$$\frac{dp}{d\tau} = \hat{k}_0 c_1 + \hat{k}_{-2} c_2 - \hat{k}_2 p(1 - c_1 - c_2), \tag{4d}$$

where

$$\varepsilon = \frac{e_0}{s_0},$$
$$\hat{k}_0 = \frac{k_0}{k_1 s_0},$$
$$\hat{k}_{-1} = \frac{k_{-1}}{k_1 s_0},$$
$$\hat{k}_2 = \frac{k_2}{k_1}, \tag{5}$$
$$\hat{k}_{-2} = \frac{k_{-2}}{k_1 s_0},$$

are dimensionless parameters.

We have omitted the equation for e here since this can be determined from the dimensionless form for (4), given by

$$e + c_1 + c_2 = 1.$$

These equations are solved subject to the initial conditions

$$\begin{aligned} e(t = 0) &= 1, \\ s(t = 0) &= 1, \\ c_1(t = 0) &= 0, \\ c_2(t = 0) &= 0, \\ p(t = 0) &= 0. \end{aligned} \tag{6}$$

In applications, the amount of substrate initially present typically greatly exceeds the enzyme present, so that $e_0 \ll s_0$. Hence, it is of value to consider the behavior of (4),(6) in the limit $\varepsilon \to 0$. There is an

initial transient at $\tau = O(\varepsilon)$ as $\varepsilon \to 0$, but this behavior is of limited practical interest, and its discussion is omitted here. For $\tau = O(1)$, we have at leading order as $\varepsilon \to 0$ that (see (4))

$$e + c_1 + c_2 = 1,$$
$$-pc_1 - (p + \hat{k}_{-2}/\hat{k}_2)c_2 + p = 0,$$
$$-(s + \hat{k}_0 + \hat{k}_{-1})c_1 - sc_2 + s = 0,$$

and these expressions may be manipulated to give

$$c_1 = \frac{s}{s + (\hat{k}_0 + \hat{k}_{-1})(1 + p\hat{k}_2/\hat{k}_{-2})},$$
$$c_2 = \frac{p}{p + (1 + s/(\hat{k}_0 + \hat{k}_{-1}))\hat{k}_{-2}/\hat{k}_2}.$$

Substituting these expressions into (4) gives

$$\frac{dp}{d\tau} = \frac{\hat{k}_0 s}{s + (\hat{k}_0 + \hat{k}_{-1})(1 + p\hat{k}_2/\hat{k}_{-2})}. \tag{7}$$

Reverting to dimensional variables, the rate of formation of product is now given by

$$v = \frac{d[P]}{dt} = k_1 e_0 s_0 \frac{dp}{d\tau} \tag{8}$$

and using (7), this leads to

$$v = \frac{d[P]}{dt} = \frac{V_{max}[S]}{[S] + K_m \left(1 + \dfrac{[P]}{K_D}\right)}, \tag{9}$$

where

$$V_{max} = k_0 e_0, \quad K_m = \frac{k_0 + k_{-1}}{k_1}, \quad K_D = \frac{k_{-2}}{k_2}.$$

Here $V_{max} = k_0 e_0$ is the maximum production rate for the enzyme, K_m is the Michaelis constant for the enzyme in the absence of product inhibition, and K_D is the dissociation constant for product binding to the enzyme. Notice that we can write (9) as

$$v = \frac{V_{max}[S]}{[S] + K_m^{app}}, \tag{10}$$

where

$$K_m^{app} = K_m \left(1 + \frac{[P]}{K_D}\right) \tag{11}$$

is the apparent Michaelis-Menten constant that takes account of competitive product inhibition. It is noteworthy here that the maximal production rate for the enzyme V_{max} is unaffected by product inhibition. However, the apparent Michaelis-Menten constant increases linearly with product concentration; see Figure 2. Figure 3 shows the Lineweaver-Burk plots of the product formation rate formula (10) for $[P] = 0$ and one value with $[P] > 0$. It can be seen that the maximal product formation rate does not depend on the product concentration, while the slope of the line corresponding to $[P] > 0$ is greater than that of the line corresponding to $[P] = 0$, as would be expected since the presence of product slows the speed of product formation.
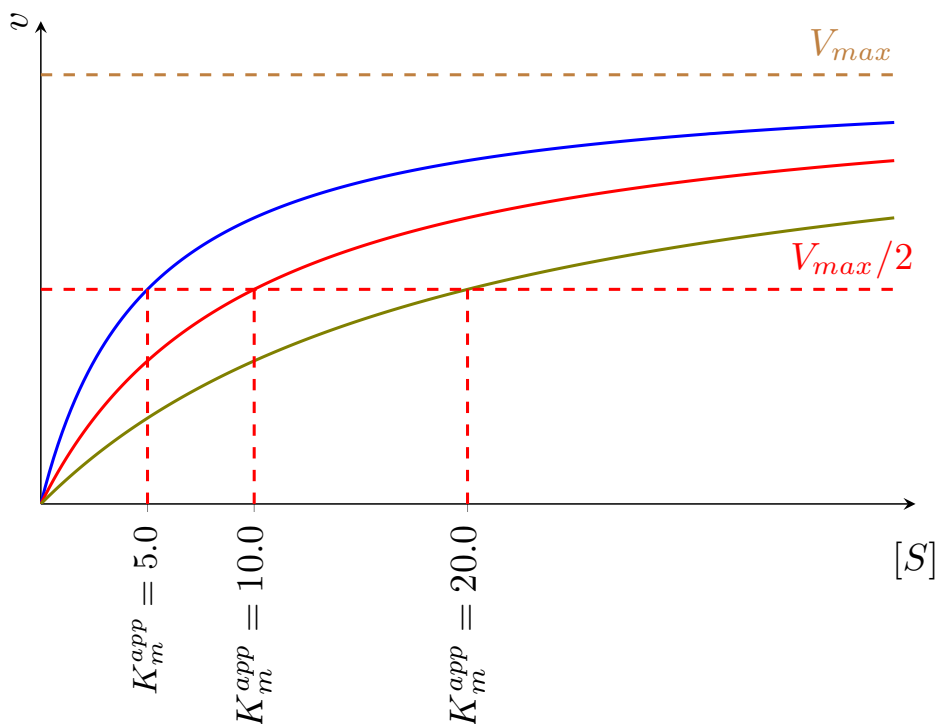
Figure 2: Plots of the rate of product formation for the case of competitive product inhibition. The relevant formula is given in equation (9), and the plots shown illustrate the effect of the product concentration on the product formation rate. The parameter values used to generate these plots are given by $V_{max} = 4.0\ mM/s$, $K_m = 5.0\ mM$, $K_D = 1.0\ mM$, and $[P] = 0.0, 1.0, 3.0\ mM$, with corresponding values $K_m^{app} = 5.0\ mM$, $K_m^{app} = 10.0\ mM$, $K_m^{app} = 20.0\ mM$, respectively.

4. The effects of the model parameters on the model output

In this section, we numerically integrate the model to study the effects of the model parameters on the output by using the `odeint` solver [12] of the module `integrate` of the `Scipy` library [13] of Python [14]. The product concentration is considered as the model output. The initial conditions used here are given by:

$$[E](t = 0) = 0.01\ mM,$$
$$[S](t = 0) = 10.0\ mM,$$
$$[P](t = 0) = 0.0\ mM,$$
$$[EP](t = 0) = 0.0\ mM,$$
$$[ES](t = 0) = 0.0\ mM,$$

and the values of model parameters are set as follows:

$$k_0 = 1000.0\ s^{-1},$$
$$k_1 = 10000.0\ mM^{-1}s^{-1}, \qquad k_{-1} = 3000.0\ s^{-1},$$
$$k_2 = 5000.0\ mM^{-1}s^{-1}, \qquad k_{-2} = 1000.0\ s^{-1}.$$

To investigate the effects of the catalytic rate constant k_0 on the output, we numerically solved the model for the three values k_0, $1.3k_0$, and $0.7k_0$, while the values of other parameters are fixed. The same process was applied to the rest of parameters. Figure 4 shows the output for the different values of k_0. The blue line corresponds to the value $k_0 = 1000.0\ s^{-1}$, the red dashed line corresponds to the value $k_0 = 1300.0\ s^{-1}$, and the green dashed-dotted line corresponds to the value $k_0 = 700.0\ s^{-1}$. It can be seen that the output is proportional to the value of k_0, that is the higher the value of k_0 is, the higher the output is.
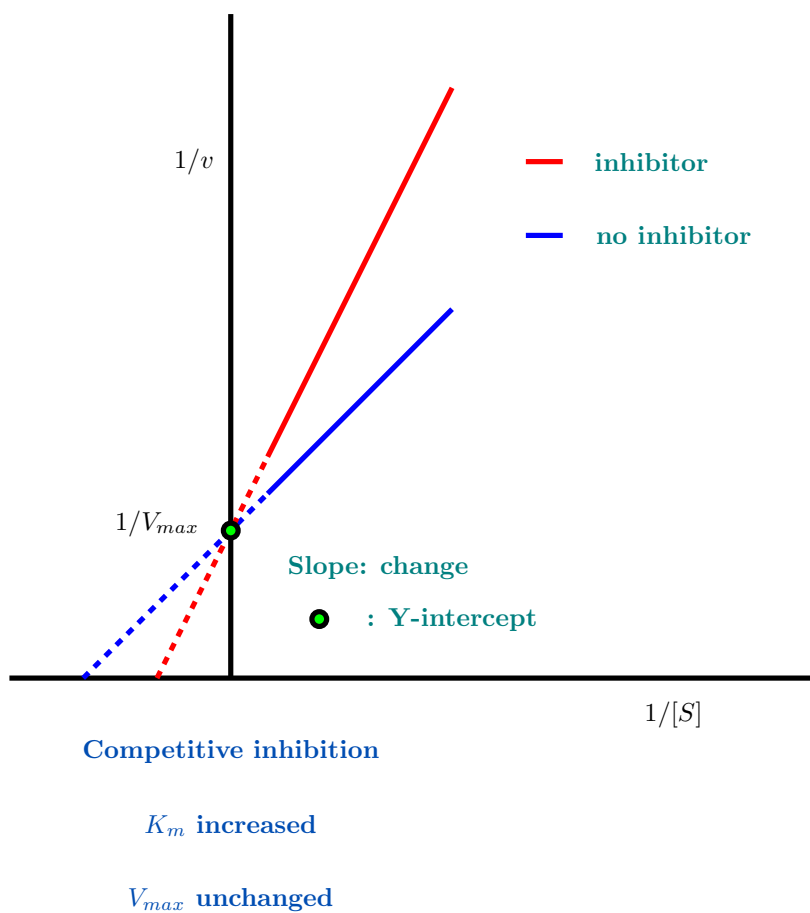
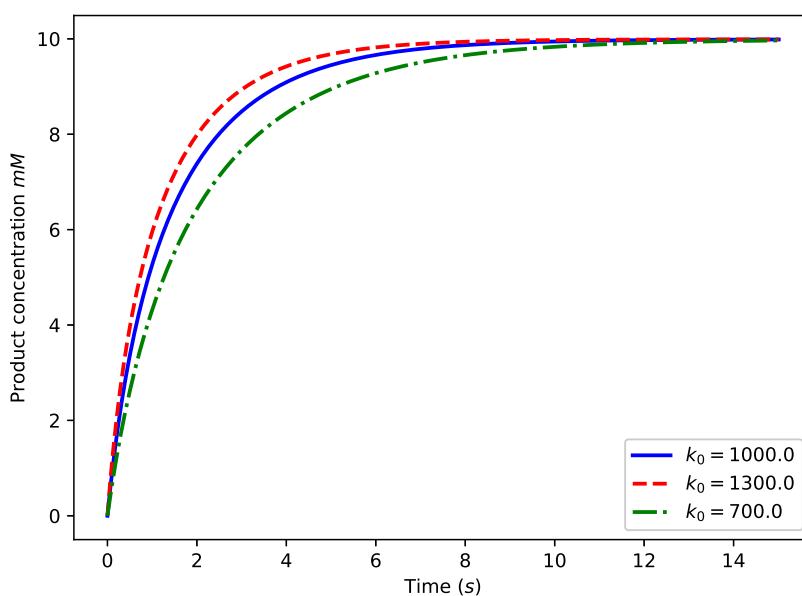Figure 3: Lineweaver-Burk plots of the product formation rate formula (10) for $[P] = 0$ and $[P] > 0$.

Figure 4: The effects of the catalytic rate constant k_0 on the model output. The blue line corresponds to the value $k_0 = 1000.0 \ s^{-1}$, the red dashed line corresponds to the value $k_0 = 1300.0 \ s^{-1}$, and the green dashed-dotted line corresponds to the value $k_0 = 700.0 \ s^{-1}$. The values of other parameters are referred to the main text.

In Figure 5, we plot concentrations of product for the different values of k_1. The blue line corresponds to the value $k_1 = 10000.0 \ mM^{-1}s^{-1}$, the red dashed line corresponds to the value $k_1 = 13000.0 \ mM^{-1}s^{-1}$, and the green dashed-dotted line corresponds to the value $k_1 = 7000.0 \ mM^{-1}s^{-1}$. It can be seen that the output is proportional to the value of k_1, that is the higher the value of k_1 is, the higher the output is.
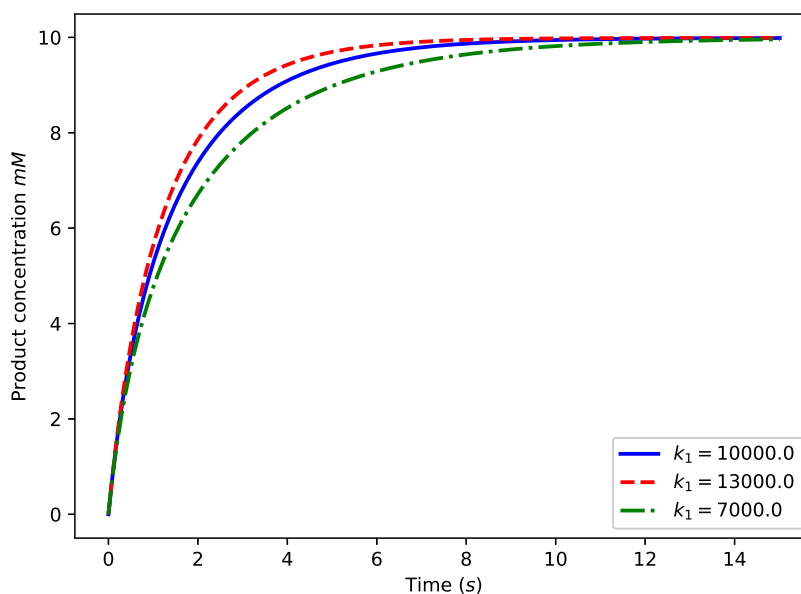

Figure 5: The effects of the binding rate constant k_1 of the product on the model output. The blue line corresponds to the value $k_1 = 10000.0 \ mM^{-1}s^{-1}$, the red dashed line corresponds to the value $k_1 = 13000.0 \ mM^{-1}s^{-1}$, and the green dashed-dotted line corresponds to the value $k_1 = 7000.0 \ mM^{-1}s^{-1}$. The values of other parameters are referred to the main text.

Figure 6 shows concentrations of product for the different values of k_2. The blue line corresponds to the value $k_2 = 5000.0 \ mM^{-1}s^{-1}$, the red dashed line corresponds to the value $k_2 = 6500.0 \ mM^{-1}s^{-1}$, and the green dashed-dotted line corresponds to the value $k_2 = 3500.0 \ mM^{-1}s^{-1}$. It can be seen that the output is inversely proportional to the value of k_2, that is the higher the value of k_2 is, the lower the output is. This implies that reducing the binding rate constant of the product to the enzyme may be a potential approach to accelerate the rate of the enzymatic reaction.

In Figure 7, we plot concentrations of product for the different values of k_{-2}. The blue line corresponds to the value $k_{-2} = 1000.0 \ s^{-1}$, the red dashed line corresponds to the value $k_{-2} = 1300.0 \ s^{-1}$, and the green dashed-dotted line corresponds to the value $k_{-2} = 700.0 \ s^{-1}$. It can be seen that the output is proportional to the value of k_{-2}, that is the higher the value of k_{-2} is, the lower the output is. This implies that increasing the unbinding rate constant of the product from the enzyme-product complex may be a potential approach to accelerate the rate of the enzymatic reaction.

In the next section, we provide a brief introduction of a potential application of the model to a real enzyme.

5. Model and glucose phosphorylation by mini-hexokinase I

Glucose glycolysis is a key pathway for the production of energy in a cell, and glycolytic intermediates form precursors for the biosynthesis of other key cellular constituents, such as glycogen, nucleotide sugars, and hyaluronan. The first step of glycolysis is the transformation of glucose into glucose-6-phosphate. This is achieved via a phosphorylation that is catalysed by an enzyme called hexokinase. There are four isozymes of hexokinase found in mammalian tissue [15, 16], and these are usually referred to as hexokinase I, II, III, and IV (glucokinase).
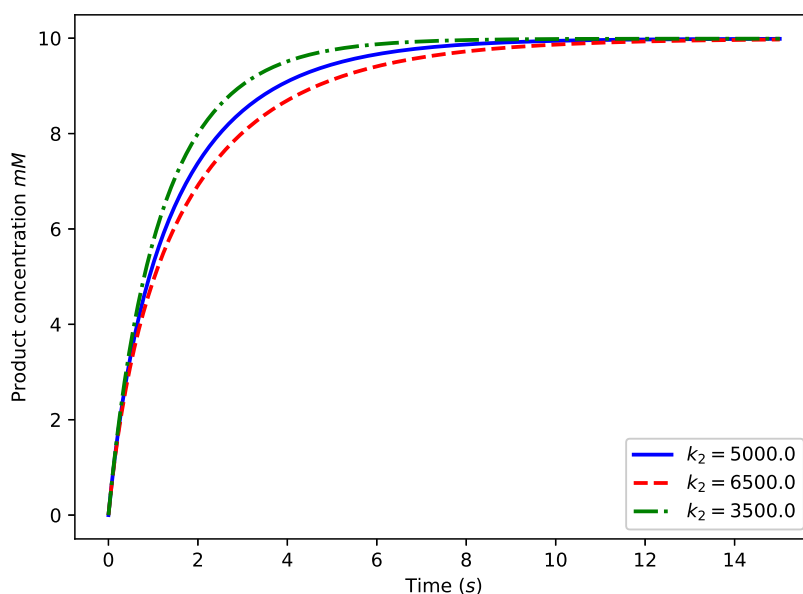
Figure 6: The effects of the binding rate constant k_2 of the product on the model output. The blue line corresponds to the value $k_2 = 5000.0 \; mM^{-1}s^{-1}$, the red dashed line corresponds to the value $k_2 = 6500.0 \; mM^{-1}s^{-1}$, and the green dashed-dotted line corresponds to the value $k_2 = 3500.0 \; mM^{-1}s^{-1}$. The values of other parameters are referred to the main text.
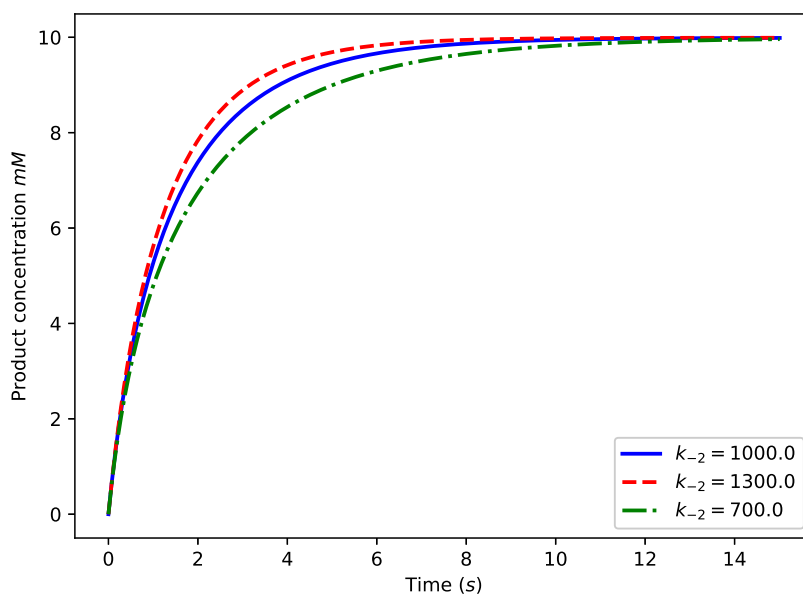

Figure 7: The effects of the binding rate constant k_{-2} of the product on the model output. The blue line corresponds to the value $k_{-2} = 1000.0 \; s^{-1}$, the red dashed line corresponds to the value $k_{-2} = 1300.0 \; s^{-1}$, and the green dashed-dotted line corresponds to the value $k_2 = 700.0 \; s^{-1}$. The values of other parameters are referred to the main text.

The product of glucose phosphorylation, glucose-6-phosphate ($G6P$), inhibits the activity of hexokinase I, II, and III [17]. Only the C domain of hexokinase I contains the catalytic site, whereas the N domain does not [6, 17, 18]. Hexokinase I has binding sites for adenosine triphosphate (ATP), glucose, and $G6P$ in both N and C domains [6, 7]. Furthermore, the binding sites for ATP and $G6P$ have a common part, so they compete together for binding sites [6].

Figure 8 represents a single hexokinase I molecule, with blue being used for the N terminal domain and green for the C terminal domain. Each hexokinase I molecule possesses binding sites for glucose, ATP, and $G6P$ in the both C and N domains, even though the C domain only is catalytically active [17, 18, 19]. In Figure 8, the binding sites for glucose on the C and N domains are depicted by the ⊔ shape, and the binding sites for ATP, glucose-6-phosphate, and inorganic phosphate are represented by a ∨ cleft.

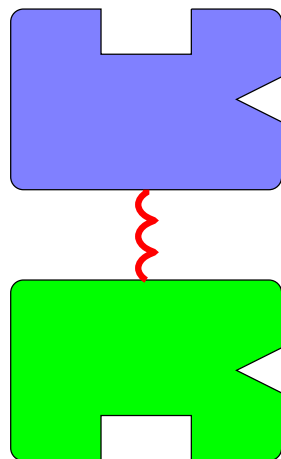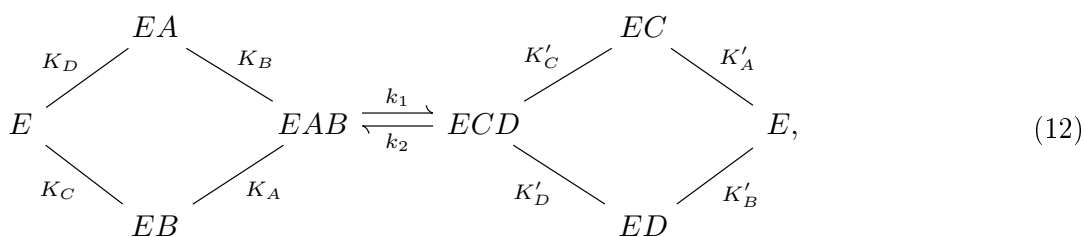
Figure 8: Schematic representation of the hexokinase I enzyme. The C and N domains are coloured green and light blue, respectively. ⊔: binding sites for glucose; ∨: binding sites for ATP and $G6P$.

In 1969, J. Ning, D. L. Purich, and H. J. Fromm [20] proposed a random Bi Bi kinetic mechanism for hexokinase I. This mechanism can be represented by the following set of chemical equations

$$
\begin{array}{ccccc}
 & EA & & EC & \\
K_D \nearrow & & \searrow K_B \quad K'_C \nearrow & & \searrow K'_A \\
E & & EAB \underset{k_2}{\overset{k_1}{\rightleftharpoons}} ECD & & E, \\
K_C \searrow & & \nearrow K_A \quad K'_D \searrow & & \nearrow K'_B \\
 & EB & & ED &
\end{array}
\tag{12}
$$

where here E, A, B, C, D represent hexokinase enzyme, ATP, glucose, adenosine diphosphate (ADP), and $G6P$, respectively. Moreover, K_X, K'_X with $X = A, B, C, D$ are the dissociation constants for the four species. Finally, k_1 and k_2 are forward and backward rate constants, respectively, for the catalytic reaction. Many investigators have found experimental evidence in support of the Bi Bi mechanism for hexokinase I [17, 21].

The model just described may be applicable to a mini-hexokinase I system. A mini-hexokinase molecule consists of the C terminal half only of the hexokinase I enzyme [19, 22], and this corresponds to the enzyme species E in our model above; see Figure 9. The active site here is the binding site for ATP, so that ATP corresponds to the substrate S in the model. The product P here is $G6P$ since $G6P$ competes with ATP for the ATP binding site. However, the correspondence between the model and the mini-hexokinase I system falls down here since $G6P$ is not a direct product of ATP binding - recall that a glucose molecule must also be bound to its site in the C terminal domain in order for $G6P$ to be formed. However, $G6P$ would be the effective product of ATP binding if ATP binding is the rate-limiting step for product formation. This would

be the case for sufficiently high concentrations of glucose, for example. The model also does not take account of phosphate binding, and so would only apply to the mini-hexokinase system if phosphate concentrations are sufficiently low. However, in these circumstances, the rate of production of $G6P$ may be approximated by (see (9))
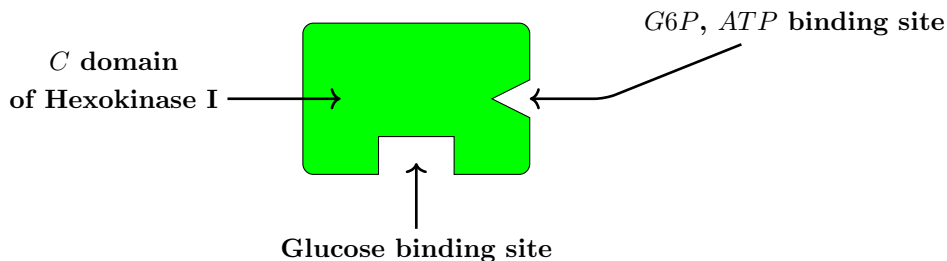

Figure 9: Mini-hexokinase I.

$$v = \frac{V_{max}[ATP]}{[ATP] + K_m^{ATP}(1 + [G6P]/K_D^{G6P})}.$$
(13)

Figure 10 displays plots of this formula for different concentrations of the product $G6P$. The parameters values used here are $k_0 = 60\ s^{-1}$, $K_m^{ATP} = 0.68\ mM$, $K_D^{G6P} = 0.05\ mM$ [23], $[HK] = 0.05\ mM$, and $[G6P] = 0.0, 0.05, 0.2\ mM$.
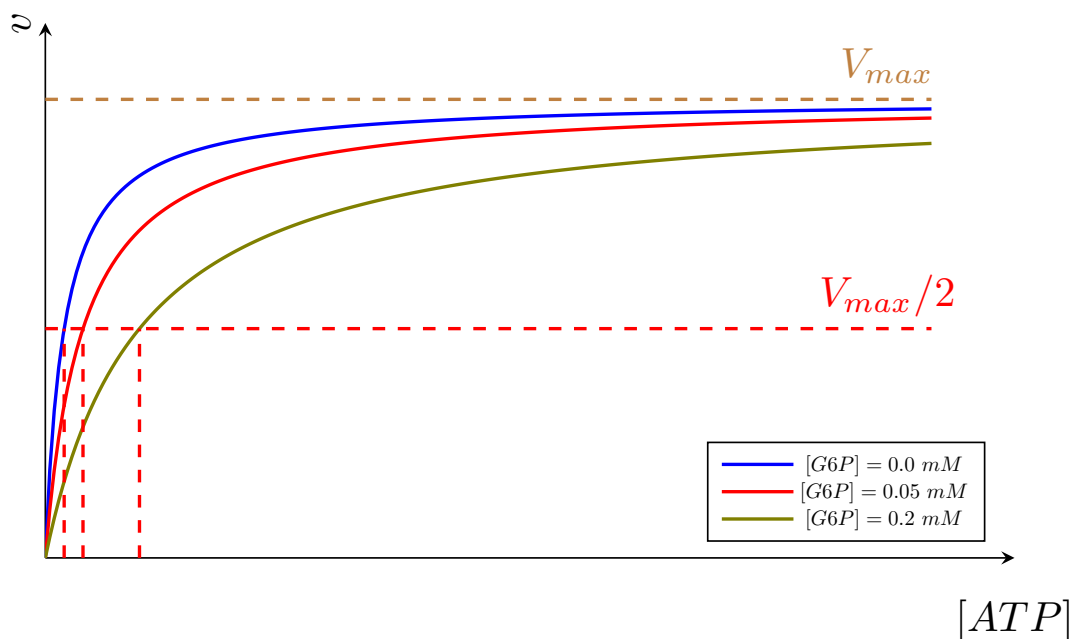

Figure 10: Plots of the product formation rate for different concentrations of product $G6P$. The relevant formula is given in equation (13). The parameters values used here are $k_0 = 60\ s^{-1}$, $K_m^{ATP} = 0.68\ mM$, $K_D^{G6P} = 0.05\ mM$, $[HK] = 0.05\ mM$, and $[G6P] = 0.0, 0.05, 0.2\ mM$.

6. Conclusions

Enzymatic competitive inhibition is one of the key regulatory mechanisms that cells use to regulate the concentrations of metabolites in physiological levels, especially the competitive product inhibition of an enzyme. Hence, from the point of view of applications, the development of reliable mathematical models for

the enzymatic competitive inhibition by product is clearly desirable. Although the formula for the product formation rate is already available in the literature [8, 9], we derive it in a transparent manner by non-dimensionalizing the equations and making rational approximations in this paper. The effects of the model parameters on the model output were investigated using a Python software to numerically integrate the model. The model was seen to model, under appropriate conditions, the phosphorylation of glucose by mini-hexokinase I. Also, the model may be applied to describe the reaction of β-galactosidase [24]. The system under consideration may be further studied in the form of fractional differential equations, such as Caputo fractional differential equations [25, 26].

Acknowledgement

References

[1] A.L. Lehninger, D.L. Nelson, M.M. Cox, Mi. M Cox, et al, Lehninger principles of biochemistry, Macmillan (2005).

[2] T.D. H. Bugg, Introduction to enzyme and coenzyme chemistry, John Wiley & Sons (2012).

[3] P.A. Frey, A.D. Hegeman, Enzymatic reaction mechanisms, Oxford University Press (2007).

[4] A. Cornish-Bowden, Fundamentals of enzyme kinetics, volume 510, Wiley-Blackwell Weinheim, Germany (2012).

[5] K.B. Taylor, Enzyme kinetics and mechanisms, Springer Science & Business Media (2002).

[6] J.E. Wilson, Isozymes of mammalian hexokinase: structure, subcellular localization and metabolic function, J. Exptl. Biol., 206(12) (2003) 2049-2057. doi:10.1242/jeb.00241

[7] X. Liu, C.S. Kim, F.T. Kurbanov, R.B. Honzatko, H.J. Fromm, Dual mechanisms for glucose 6-phosphate inhibition of human brain hexokinase, J. Biol. Chem., 274(44) (1999) 31155-31159. doi:10.1074/jbc.274.44.31155

[8] I.H. Segel, Enzyme kinetics: behavior and analysis of rapid equilibrium and steady state enzyme systems, Wiley New York (1993).

[9] B.P. Ingalls, Mathematical modeling in systems biology: an introduction, MIT Press (2013).

[10] D. Fell, A. Cornish-Bowden. Understanding the control of metabolism, volume 2, Portland Press London (1997).

[11] V. Q. Mai, T. T. Vo, M. Meere, Modelling hyaluronan degradation by streptococcus pneumoniae hyaluronate lyase, J. Math. Biosci, 303 (2018) 126-138. doi:10.1016/j.mbs.2018.07.002

[12] The odeint solver in the integrate module of the scipy library. https://docs.scipy.org/doc/scipy/reference/generated/scipy.integrate.odeint.html, Accessed: 2020-9-25.

[13] Scipy open source python library, https://www.scipy.org/, Accessed: 2020-9-25.

[14] Python software foundation, https://www.python.org/, Accessed: 2020-9-25.

[15] H.M. Katzen, R.T. Schimke, Multiple forms of hexokinase in the rat: tissue distribution, age dependency, and properties. Proc. Natl. Acad Sci., 54(4) (1965) 1218-1225. doi:10.1073/pnas.54.4.1218

[16] V. Stocchi, M. Magnani, F. Canestrari, M. Dacha, G. Fornaini, Multiple forms of human red blood cell hexokinase. preparation, characterization, and age dependence, J. Biol. Chem., 257(5) (1982) 2357-2364.

[17] J. E. Wilson, Hexokinases. Reviews of physiology, biochemistry and pharmacology, 126 (1995) 65. doi:10.1007/BFb0049776

[18] T.K. White, J.E. Wilson, Isolation and characterization of the discrete N- and C-terminal halves of rat brain hexokinase: retention of full catalytic activity in the isolated C-terminal half, Arch. Biochem. Biophys., 274(2) (1989) 375-393. https://doi.org/10.1016/0003-9861(89)90451-7

[19] K.K. Arora, C.R. Filburn, P.L. Pedersen, Structure/function relationships in hexokinase. Site-directed mutational analyses and characterization of overexpressed fragments implicate different functions for the N- and C-terminal halves of the enzyme, J. Biol. Chem., 268(24) (1993) 18259-18266.

[20] J. Ning, D. L. Purich, H. J. Fromm, Studies on the kinetic mechanism and allosteric nature of bovine brain hexokinase, J. Biol. Chem., 244(14) (1969) 3840-846.

[21] G. Gerber, H. Preissler, R. Heinrich, S.M. Rapoport, Hexokinase of human erythrocytes: purification, kinetic model and its application to the conditions in the cell, Eur. J. Biochem., 45(1) (1974) 39-52. doi:10.1111/j.1432-1033.1974.tb03527.x

[22] C. Zeng, H.J. Fromm, Active site residues of human brain hexokinase as studied by site-specific mutagenesis, J. Biol. Chem., 270(18) (1995) 10509-10513. doi:10.1074/jbc.270.18.10509

[23] T.Y. Fang, O. Alechina, A.E. Aleshin, H.J. Fromm, R.B. Honzatko, Identification of a phosphate regulatory site and a low affinity binding site for glucose 6-phosphate in the N-terminal half of human brain hexokinase. J. Biol. Chem., 273(31) (1998) 19548-19553. doi:10.1074/jbc.273.31.19548

[24] Z. Zhang, F. Zhang, L. Song, N. Sun, W. Guan, B. Liu, J. Tian, Y. Zhang, W. Zhang, Site-directed mutation of β-alactosidase from aspergillus candidus to reduce galactose inhibition in lactose hydrolysis, 3 Biotech., 8(11) (2018) 452. doi:10.1007/s13205-018-1418-5

[25] J. Patil, A. Chaudhari, M.S. Archana, M.S. Abdo, B. Hardan, Upper and lower solution method for positive solution of generalized caputo fractional differential equations. Advances in the Theory of Nonlinear Analysis and its Application, 4(4) (2020) 279-291. https://doi.org/10.31197/atnaa.709442

[26] S.S. Redhwan, S.L. Shaikh, M.S. Abdo, Some properties of sadik transform and its applications of fractional-order dynamical systems in control theory, arXiv preprint arXiv:1912.11484 (2019).